Coupling effect between two adjacent chiral structure layers

Zhaofeng Li[1]*, Humeyra Caglayan[1], Evrim Colak[1], Jiangfeng Zhou[2], Costas M. Soukoulis[2,3], and Ekmel Ozbay[4]

[1] Nanotechnology Research Center, and Department of Physics, Bilkent University, Bilkent, 06800 Ankara, Turkey
[2] Department of Physics and Astronomy and Ames Laboratory, Iowa State University, Ames, Iowa 50011, USA
[3] Institute of Electronic Structure and Laser, Foundation for Research and Technology Hellas (FORTH), and Department of Materials Science and Technology, University of Crete, 71110 Heraklion, Greece
[4] Nanotechnology Research Center, Department of Physics, and Department of Electrical and Electronics Engineering, Bilkent University, Bilkent, 06800 Ankara, Turkey
*zhaofengli@bilkent.edu.tr

Abstract: A pair of mutually twisted metallic cross-wires can produce giant optical activity. When this single chiral layer is stacked layer by layer in order to build a thick chiral metamaterial, strong coupling effects are found between the two adjacent chiral layers. We studied these coupling effects numerically and experimentally. The results show that the existing coupling between chiral layers can make the chiral properties of a two-layered chiral metamaterial different from the constituting single chiral layers. It is explained qualitatively that the coupling effects are generated from the coupling of metallic cross-wires belonging to different chiral layers. Our experimental results are in good agreement with the simulation results.

References and links

1. D. Schurig, J. J. Mock, B. J. Justice, S. A. Cummer, J. B. Pendry, A. F. Starr, and D. R. Smith, "Metamaterial electromagnetic cloak at microwave frequencies," Science **314**(5801), 977–980 (2006).
2. K. Aydin, K. Guven, M. Kafesaki, L. Zhang, C. M. Soukoulis, and E. Ozbay, "Experimental observation of true left-handed transmission peaks in metamaterials," Opt. Lett. **29**(22), 2623–2625 (2004).
3. I. Bulu, H. Caglayan, and E. Ozbay, "Highly directive radiation from sources embedded inside photonic crystals," Appl. Phys. Lett. **83**(16), 3263–3265 (2003).
4. J. B. Pendry, A. J. Holden, D. J. Robbins, and W. J. Stewart, "Magnetism from Conductors and Enhanced Nonlinear Phenomena," IEEE Trans. Microw. Theory Tech. **47**(11), 2075–2084 (1999).
5. D. R. Smith, W. J. Padilla, D. C. Vier, S. C. Nemat-Nasser, and S. Schultz, "Composite medium with simultaneously negative permeability and permittivity," Phys. Rev. Lett. **84**(18), 4184–4187 (2000).
6. K. Aydin, A. O. Cakmak, L. Sahin, Z. Li, F. Bilotti, L. Vegni, and E. Ozbay, "Split-ring-resonator-coupled enhanced transmission through a single subwavelength aperture," Phys. Rev. Lett. **102**(1), 013904 (2009).
7. H. J. Lezec, A. Degiron, E. Devaux, R. A. Linke, L. Martin-Moreno, F. J. Garcia-Vidal, and T. W. Ebbesen, "Beaming light from a subwavelength aperture," Science **297**(5582), 820–822 (2002).
8. Z. Li, K. B. Alici, H. Caglayan, and E. Ozbay, "Generation of an axially asymmetric Bessel-like beam from a metallic subwavelength aperture," Phys. Rev. Lett. **102**(14), 143901 (2009).
9. J. B. Pendry, "Negative refraction makes a perfect lens," Phys. Rev. Lett. **85**(18), 3966–3969 (2000).
10. K. Aydin, K. Guven, N. Katsarakis, C. M. Soukoulis, and E. Ozbay, "Effect of disorder on magnetic resonance band gap of split-ring resonator structures," Opt. Express **12**(24), 5896–5901 (2004).
11. M. Gokkavas, K. Guven, I. Bulu, K. Aydin, R. S. Penciu, M. Kafesaki, C. M. Soukoulis, and E. Ozbay, "Experimental demonstration of a left-handed metamaterial operating at 100 GHz," Phys. Rev. B **73**(19), 193103 (2006).
12. G. Dolling, C. Enkrich, M. Wegener, J. F. Zhou, C. M. Soukoulis, and S. Linden, "Cut-wire pairs and plate pairs as magnetic atoms for optical metamaterials," Opt. Lett. **30**(23), 3198–3200 (2005).
13. M. Kafesaki, I. Tsiapa, N. Katsarakis, T. Koschny, C. M. Soukoulis, and E. N. Economou, "Left-handed metamaterials: The fishnet structure and its variations," Phys. Rev. B **75**(23), 235114 (2007).
14. K. Aydin, Z. Li, L. Sahin, and E. Ozbay, "Negative phase advance in polarization independent, multi-layer negative-index metamaterials," Opt. Express **16**(12), 8835–8844 (2008).
15. L. Jylhä, I. Kolmakov, S. Maslovski, and S. Tretyakov, "Modeling of isotropic backward-wave materials composed of resonant spheres," J. Appl. Phys. **99**(4), 043102 (2006).

16. J. Zhou, T. Koschny, M. Kafesaki, E. N. Economou, J. B. Pendry, and C. M. Soukoulis, "Saturation of the magnetic response of split-ring resonators at optical frequencies," Phys. Rev. Lett. **95**(22), 223902 (2005).
17. V. M. Shalaev, "Optical negative-index metamaterials," Nat. Photonics **1**(1), 41–48 (2007).
18. J. B. Pendry, "A chiral route to negative refraction," Science **306**(5700), 1353–1355 (2004).
19. S. Tretyakov, I. Nefedov, A. Sihvola, S. Maslovski, and C. Simovski, "Waves and Energy in Chiral Nihility," J. Electromagn. Waves Appl. **17**(5), 695–706 (2003).
20. A. V. Rogacheva, V. A. Fedotov, A. S. Schwanecke, and N. I. Zheludev, "Giant gyrotropy due to electromagnetic-field coupling in a bilayered chiral structure," Phys. Rev. Lett. **97**(17), 177401 (2006).
21. B. Wang, T. Koschny, and C. M. Soukoulis, "Wide-angle and polarization-independent chiral metamaterial absorber," Phys. Rev. B **80**(3), 033108 (2009).
22. B. Wang, J. Zhou, T. Koschny, and C. M. Soukoulis, "Nonplanar chiral metamaterials with negative index," Appl. Phys. Lett. **94**(15), 151112 (2009).
23. S. Zhang, Y.-S. Park, J. Li, X. Lu, W. Zhang, and X. Zhang, "Negative refractive index in chiral metamaterials," Phys. Rev. Lett. **102**(2), 023901 (2009).
24. J. Zhou, J. Dong, B. Wang, T. Koschny, M. Kafesaki, and C. M. Soukoulis, "Negative refractive index due to chirality," Phys. Rev. B **79**(12), 121104 (2009).
25. E. Plum, J. Zhou, J. Dong, V. A. Fedotov, T. Koschny, C. M. Soukoulis, and N. I. Zheludev, "Metamaterial with negative index due to chirality," Phys. Rev. B **79**(3), 035407 (2009).
26. M. Decker, M. Ruther, C. E. Kriegler, J. Zhou, C. M. Soukoulis, S. Linden, and M. Wegener, "Strong optical activity from twisted-cross photonic metamaterials," Opt. Lett. **34**(16), 2501–2503 (2009).
27. C. R. Simovski, "Bloch material parameters of magneto-dielectric metamaterials and the concept of Bloch lattices," Metamaterials (Amst.) **1**(2), 62–80 (2007).
28. D. R. Smith, S. Schultz, P. Markos, and C. M. Soukoulis, "Determination of effective permittivity and permeability of metamaterials from reflection and transmission coefficients," Phys. Rev. B **65**(19), 195104 (2002).
29. J. D. Jackson, *Classical Electrodynamics*, 3rd ed. (Wiley, New York, 1998).
30. J. A. Kong, *Electromagnetic Wave Theory* (EMW Publishing, Cambridge, MA, 2008).
31. D. H. Kwon, D. H. Werner, A. V. Kildishev, and V. M. Shalaev, "Material parameter retrieval procedure for general bi-isotropic metamaterials and its application to optical chiral negative-index metamaterial design," Opt. Express **16**(16), 11822–11829 (2008).
32. C. Menzel, C. Rockstuhl, T. Paul, and F. Lederer, "Retrieving effective parameters for quasiplanar chiral metamaterials," Appl. Phys. Lett. **93**(23), 233106 (2008).

1. Introduction

Metamaterials are artificially structured materials that may possess electromagnetic properties not existing in natural materials. Metamaterials can be composed of dielectric elements or structured metallic components. A lot of novel applications can be realized by using metamaterials, e.g., cloaking [1], negative refraction [2], and beaming effect [3]. Traditional metamaterials are composed of continuous metallic wires and split ring resonators (SRRs) [4,5]. It is found recently that SRRs can even be used to enhance the transmission of electromagnetic waves through a subwavelength aperture [6] from which beaming effect can be generated [7,8]. Since Pendry proposed that a perfect lens can be realized with negative index metamaterials (NIMs) [9], studies regarding NIMs have attracted much attention and effort from scientific researchers. NIMs have been realized in artificial structures that consist of continuous metallic wires and split ring resonators (or cut-wire pairs), fishnet structures, and dielectric resonators [2,5,10–15]. In all of these NIMs, a negative index is obtained by adjusting the permittivity and permeability to be negative simultaneously. Although negative permeability (using split ring resonators) can be easily obtained in the microwave frequency range, that is not the case in the optical frequency range [16,17]. Recently, it has been proposed that a negative index can be achieved alternatively through a chiral route [18,19]. A chiral material lacks any mirror symmetry. This results in the breaking of the degeneracy of two circularly polarized waves, i.e. right circularly polarized (RCP) waves and left circularly polarized (LCP) waves have different refractive indices. Given a strong enough chirality, it is possible to obtain a negative index for one circularly polarized wave while the permittivity and permeability remain positive. There have been several reports on the investigation of chiral metamaterials [20–26] that vary from two-dimensional (2D) planar structures to three-dimensional structures. However, considering the possible nanofabrication of such structures operating in the optical frequency range, 2D planar chiral structures are thought to be more compatible with the well-established planar technology. In fact, several planar chiral structures have been proposed that consist of bilayered rosettes or cross-wires [20,24–26].

Negative indices were claimed to be obtained due to the very large chirality obtained from these structures [24,25].

A straightforward way to construct a bulk chiral metamaterial is to stack the planar chiral structures layer by layer periodically. However, as has been pointed out by Simovski [27], the bulk metamaterials that are stacked in this way may have properties varied from single layered components due to the coupling effect between the individual layers. For instance, the transmission properties of bulk metamaterials cannot be described by multiplying the transfer matrix of the single layered component. This kind of metamaterial is called a non-Bloch metamaterial, for which a conventional retrieval procedure [28] (using the transmission and reflection coefficients of a single layer structure) cannot provide meaningful effective parameters for the desired bulk chiral metamaterial. A similar situation might occur to the planar chiral structures. To address this problem, in the present paper we numerically and experimentally study the transmission properties of planar chiral structures with a one-layered sample and a series of two-layered samples with different distances between them.

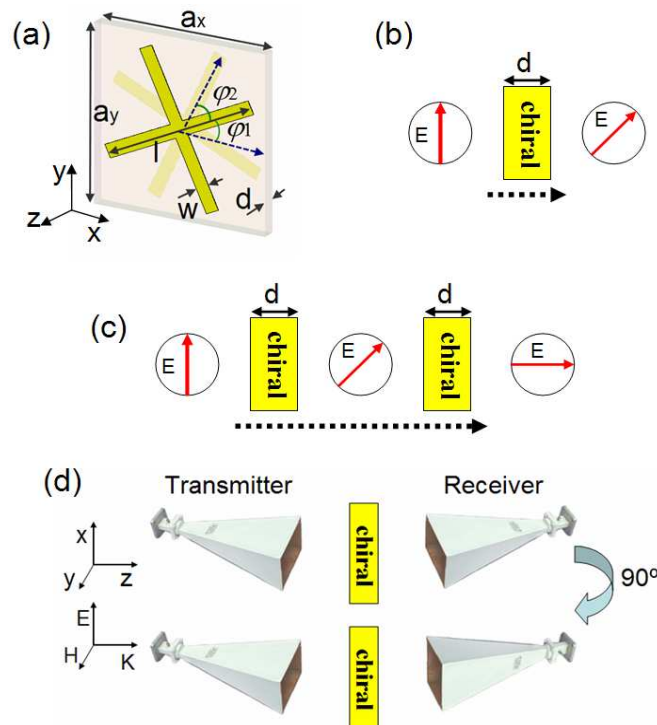## 2. The chiral structure consisting of cross-wire pair

Fig. 1. (a) Schematic of one unit cell of the cross-wire chiral structure. The geometry parameters are $a_x = a_y = 13$ mm, $l = 12$ mm, $w = 1$ mm, $d = 1$ mm, $\varphi_1 = 25°$, $\varphi_2 = 40°$. The thickness of the copper is 30 μm. (b) Schematic of a linear polarized wave transmitting through a single layer chiral metamaterial. (c) Schematic of a linear polarized wave transmitting through a two-layered chiral metamaterial. (d) Schematic of the measurement method in our experiment.

Figure 1(a) shows one unit cell of the chiral structures under study, which looks similar to that reported in Ref [24]. We have modified the structure of Ref [24]. a little so that the structure looks the same along the two directions of the + z and –z axes. The chiral structure consists of two copper cross-wires patterned on opposite sides of a Teflon dielectric board. The dielectric constant of the Teflon board is $\varepsilon_r = 2.08$ with a dielectric loss tangent of 0.0004. The detailed dimensions of the structure can be found in the caption of Fig. 1.

When an electromagnetic (EM) wave is incident on the planar structure in the direction of the $+z$ axis, the wave propagation in such a chiral structure obeys the following constitutive relations,

$$\begin{pmatrix} D \\ B \end{pmatrix} = \begin{pmatrix} \varepsilon_0 \varepsilon_r & -i\kappa/c \\ i\kappa/c & \mu_0 \mu_r \end{pmatrix} \begin{pmatrix} E \\ H \end{pmatrix} \qquad (1)$$

where ε_0 and μ_0 are the permittivity and permeability of vacuum. ε_r and μ_r are the relative permittivity and permeability of the chiral medium. c is the speed of light in vacuum. κ is the chirality. Assuming a time dependence of $e^{-i\omega t}$, the RCP (+) wave and LCP (-) wave are defined as $E^{\pm} = \frac{1}{2} E_0 (\hat{x} \mp i\hat{y})$ [29]. After some deduction [30], one obtains the refractive index for RCP and LCP waves,

$$n^{\pm} = \sqrt{\varepsilon_r \mu_r} \pm \kappa \qquad (2)$$

At the same time, both RCP and LCP waves have the same impedance of $z/z_0 = \sqrt{\mu_r/\varepsilon_r}$, where z_0 is the impedance of the vacuum.

In order to study the transmission behaviors of the chiral structures, we carried out simulation and experimental works, in which a linearly polarized EM wave (E field in x direction) is incident on the chiral structure. On the other side of the structure, we measured the transmitted field in the x and y directions (T_{xx} and T_{yx}). Figure 1(d) shows the schematic of the measurement method. Due to the fourfold rotational symmetry, circular polarization conversion is absent. The transmission of circularly polarized waves can be converted from the linear transmission coefficients T_{xx} and T_{yx} [24,31],

$$T^{\pm} = T_{xx} \pm iT_{yx} \qquad (3)$$

For the EM wave transmitted, the polarization rotation angle θ can be calculated as $\theta = [\arg(T^+) - \arg(T^-)]/2$, and the ellipticity of the transmitted wave is $\eta = \arctan[(|T^+| - |T^-|)/(|T^+| + |T^-|)]$.

Figure 1(b) shows a schematic of an EM wave propagating through a single layer of chiral materials with the incident wave being linearly polarized. The transmission of RCP and LCP waves can be calculated as the following [32],

$$T^{\pm} = Te^{\pm ik_0 \kappa d} \qquad (4)$$

where T is the transmission coefficient for $\kappa = 0$. k_0 is the wave vector of the EM wave in vacuum, and d is the thickness of the chiral material. It is easy to check that the polarization rotation angle $\theta_1 = k_0 \kappa d$.

Figure 1(c) shows a schematic of an EM wave propagating through two layers of chiral material with the incident wave being linearly polarized. If there are no coupling effects between the two chiral material layers, the chirality of the chiral material layer will remain as κ and the space between the two chiral material layers possesses no chirality. Accordingly, the transmission of the RCP and LCP waves can be calculated as the following,

$$T^{\pm} = Te^{\pm i2k_0 \kappa d} \qquad (5)$$

Obviously, with two layers of chiral material, the polarization rotation angle is $\theta_2 = 2k_0 \kappa d$, which is exactly the sum of the rotation angles of two individual chiral layers. It is noteworthy that this rotation angle is independent of the distance between the two layers of chiral materials. Thus, we obtain the criteria to judge whether there exists a coupling effect between the two layers of chiral metamaterials. If the polarization rotation angle of two chiral layers is equal to twice the rotation angle of a single chiral layer, it implies that the chirality of the

chiral layers and the interspace between the layers remains unchanged in the two-layered chiral structure. Otherwise, the chirality of the layers and/or the space between the layers must have changed due to the coupling effect between two chiral layers.

3. Results of simulation and experiments

In order to study the behaviors of the chiral structures, we conducted numerical simulation and experiments. The simulation works were carried out by using CST microwave studio (Computer Simulation Technology GmbH, Darmstadt, Germany) wherein the finite integration technique was applied. During the simulations, the periodic boundary conditions were applied to the x and y directions, and the absorbing boundary conditions were applied to the z direction. In the experiment, we fabricated the chiral structures with a dimension of 25 by 25 unit cells. The transmission coefficient was measured by an HP-8510C network analyzer with two standard horn antennas. Figure 2 shows the simulation and experimental results for a single layered chiral structure. Figure 2(a) shows the transmission spectra of RCP and LCP waves, and Fig. 2(b) shows the polarization rotation angle θ_1. The ripples on the experimental data curves in Fig. 2(a) come from the multiple reflections between the chiral structure and the horn antennas. It can be clearly seen that the transmission of RCP and LCP waves are nearly equal at all frequencies. Therefore, circular dichroism is very weak in our chiral structures, and the value of η is close to zero. This behavior is quite different from the results reported in Ref [24]. This is because the loss of our dielectric board is much lower than that in Ref [24]. From Fig. 2(b), it is seen that the polarization rotation angle reaches maximum at two frequencies $f = 10.6$ and 10.9 GHz, which corresponds to the magnetic and electric resonances [24,25], respectively. Since we are concentrating on the polarization rotation angles of the chiral structure in the present paper, the ellipticity of the transmitted wave η is not shown here.
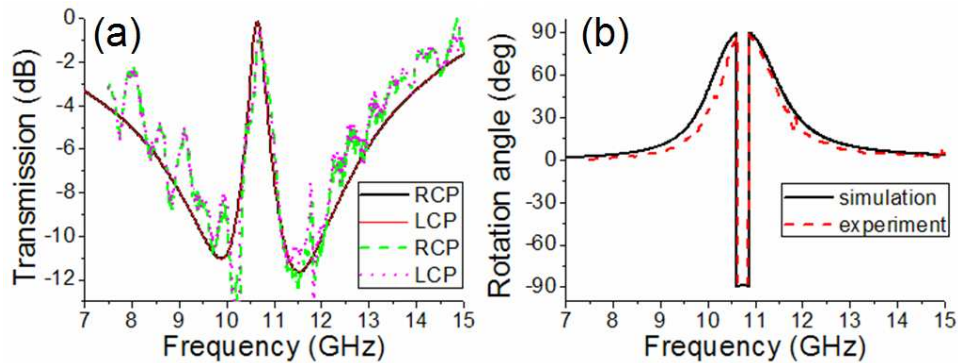

Fig. 2. (a) The transmission spectra of RCP and LCP waves through a single chiral layer. The solid lines are the simulation results. Dashed and dotted lines are the experimental results. (b) The simulation and experimental results of the polarization rotation angle.
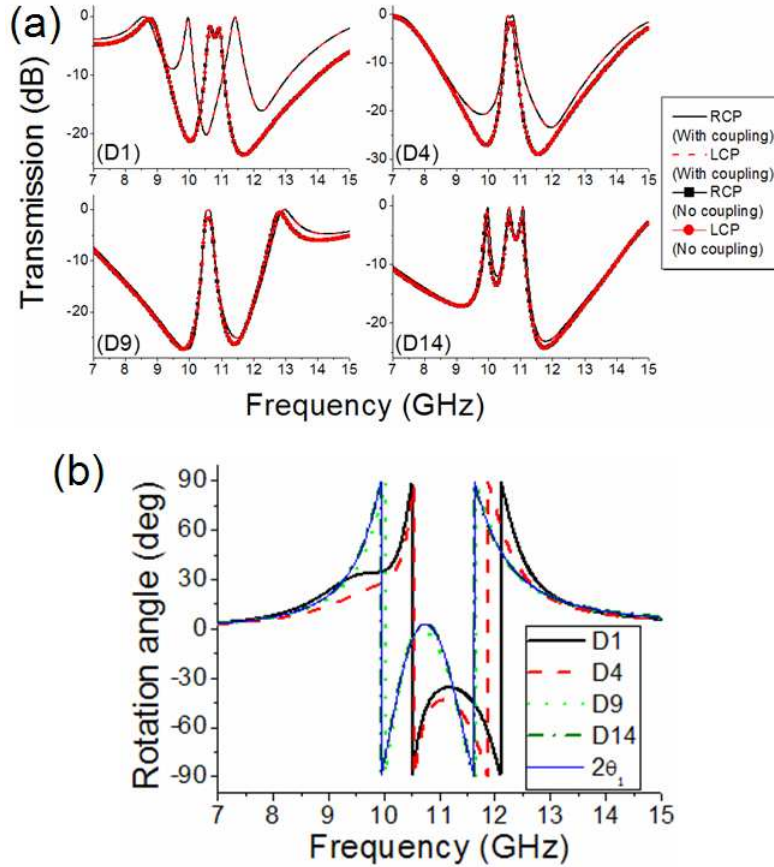
Fig. 3. Simulation results: (a) The transmission spectra of RCP and LCP waves through two chiral layers for four different configurations and their reference cases in which no coupling effect is considered; (b) The polarization rotation angle of two chiral layers and the doubled polarization rotation angle of a single chiral layer.

In order to study the possible coupling effect in a two-layered chiral structure, we arranged these two layers in a series of configurations in our simulations, i.e., the distance between the two layers were set as 1, 4, 9, and 14 mm (for convenience, these four configurations were denoted as D1, D4, D9, and D14). Figure 3(a) shows the transmission spectra of the RCP and LCP waves for these four configurations calculated by using CST microwave studio. In Fig. 3(a), we also show the transmission data for a series of reference chiral structures calculated with transfer matrix method. These reference structures are composed of two effective chiral layers, and between them no coupling effect is considered. The effective chiral layers have an effective thickness of 2 mm, and effective parameters $n^{\pm}$ and z that are retrieved [25,31] from the transmission and reflection data of a single layer of the cross-wire chiral structure [Fig. 1(a)]. Obviously, there is significant difference between the transmission spectra of D1 configuration and its reference case. With the increase of the distance between the two chiral layers, the differences of transmission spectra between the two-layered chiral structure and their references become smaller. At last, the transmission spectra of D14 are very similar to that of its reference structure. Figure 3(b) shows the polarization rotation angles for the four configurations. For the convenience of comparison, the polarization rotation angle data of a single layered chiral structure is doubled and shown in Fig. 3(b). All of the rotation angle data was normalized into domain [-90°, 90°]. From the data shown in Fig. 3(b), one can see that the rotation angle of configuration D14 is in good agreement with the doubled rotation angle of a single layered chiral structure. However, this agreement does

not hold for the other three configurations. Moreover, the closer the two chiral structure layers are, the larger the discrepancy is. These results imply that there exists coupling effects between two chiral structure layers, which can modify the chirality and transmission properties of the single chiral layer and/or the interspace between the two chiral layers when the distance between the two chiral layers is small (e.g. less than 9mm or $\lambda/3$, where λ corresponds to the wavelength of magnetic resonance). Furthermore, the coupling effects become stronger when the distance between the two chiral layers becomes smaller. When the distance between the two chiral layers increases to 14 mm (approx. $\lambda/2$), the coupling effects decline to a very weak level. Since the period constants of most metamaterials are less than 1/6 of the operation wavelength (here, less than 5 mm), one must consider the strong coupling effects when constructing a chiral metamaterial with multilayer cross-wire chiral structures. Actually, our simulation studies (not shown here) show that similar coupling effects also exist in other planar chiral metamaterials, for instance, bilayered rosettes [20,25]. Therefore, the strong coupling effects between two adjacent chiral layers are quite general phenomena that one must take into account in designing a planar chiral metamaterials.
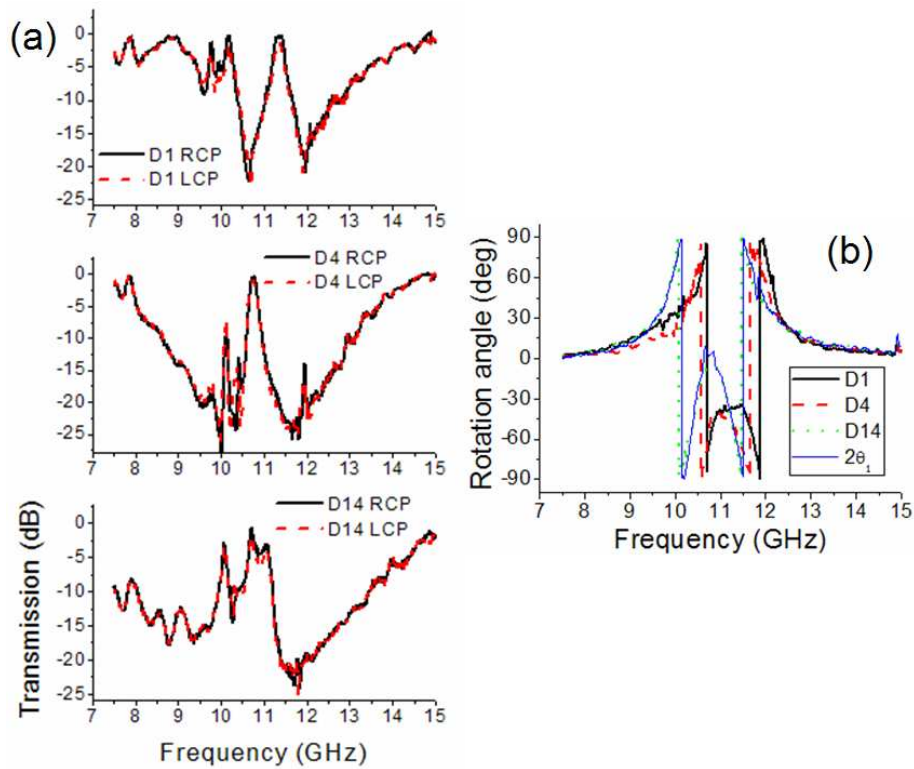

Fig. 4. Experimental results: (a) The transmission spectra of RCP and LCP waves through two chiral layers for three different configurations; (b) The polarization rotation angle of two chiral layers and the doubled polarization rotation angle of a single chiral layer.

Figure 4 shows the experimental results for the two-layered chiral metamaterial. For the sake of conciseness, we show the experimental results of only three configurations (D1, D4, and D14). Figure 4(a) shows the transmission spectra of the RCP and LCP waves, and Fig. 4(b) shows the polarization rotation angles for the three configurations, and again, the rotation angle of a single chiral layer is doubled and included in the same figure. From Fig. 4(b), it can be clearly seen that only configuration D14 has its polarization rotation angle equal to the doubled rotation angle of a single chiral layer. Our experimental results are in good agreement with our simulation results.

Based on the simulation and experimental results, it can be concluded that when the two layers of a chiral structure are closely placed, these two chiral layers will couple with each other. The coupling effects can affect the chirality of the entire chiral metamaterial. Then, how do the coupling effects arise? To answer this question, we studied the two-layered chiral metamaterial in more detail. It is already known that the chirality of the single layered chiral structure comes from the coupling of the mutually twisted two metallic cross-wires [24]. Along this line of thinking, the two-layered chiral metamaterial can be seen as consisting of four cross-wires. In Fig. 5(a), we denote these four cross-wires as W1, W2, W3, and W4. Obviously, in the two-layered chiral metamaterial, not only the coupling between W1 and W2 (or W3 and W4) gives rise to chirality, but also the coupling between W2 and W3 (or even W1 and W4) contributes to the chirality of the entire structure. Noting that the distance between W1 and W4 is much larger than that between W2 and W3, the chirality generated from the coupling of W1 and W4 should be much weaker compared to that from W2 and W3. Thus, we primarily studied the coupling effect between W2 and W3.
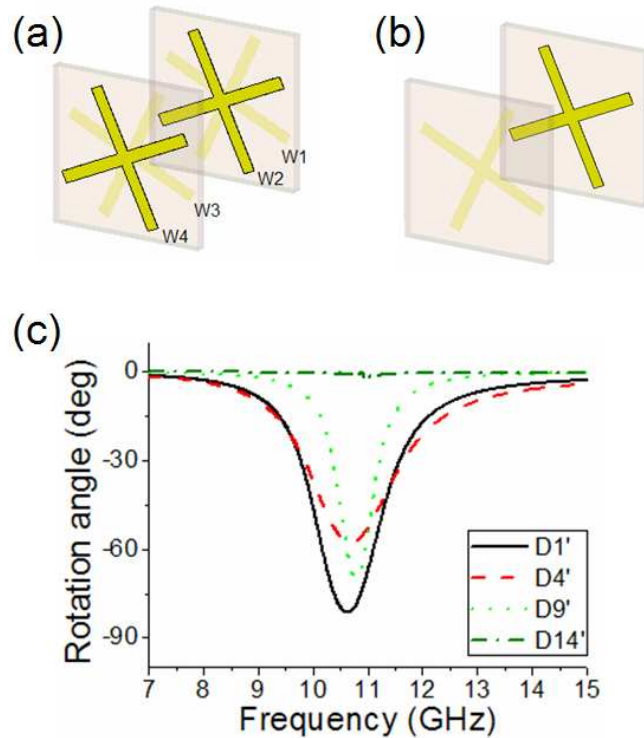

Fig. 5. (a) The schematic of a two-layered chiral metamaterial that consists of four cross-wires. (b) The schematic of a modified configuration consisting of W2 and W3 cross-wires. (c) The polarization rotation angles for four modified configurations (coupling of W2 and W3).

After removing the cross-wires W1 and W4 from the former four configurations (D1, D4, D9, and D14) of the two-layered chiral metamaterials, we obtained the corresponding four new configurations (D1', D4', D9', and D14') only with the cross-wires W2 and W3. Figure 5(b) is a schematic of the new configuration D14'. Figure 5(c) shows the simulation results of the polarization rotation angles for the four new configurations with W2 and W3. It can be clearly seen that the coupling between W2 and W3 also results in chirality. Especially in the configuration of D1', the chirality is quite strong over a broad frequency range. As the distance between W2 and W3 increases, the chirality in the configuration of D2' and D3′ becomes weaker and only affects a narrower frequency band. When the distance reaches 14 mm (approx. $\lambda/2$) in the configurations of D14', the chirality only appears with a very small

scale in the close vicinity of the electric resonant frequency. Compared with the chirality that we obtained from the single layered chiral metamaterial (coupling between W1 and W2) in Fig. 2, the chirality coming from W2 and W3 has an opposite sign at most frequencies. These opposite chiralities can counteract with each other so that the total chiral properties of the two-layered chiral metamaterials (configurations D1, D4, and D9) deviate from the summation of the constituting single chiral layers. Based on the abovementioned results, it is clear that the coupling between W2 and W3 has modified the chiral properties of the interspace between the two chiral layers. Similarly, the coupling between W1 and W4 could also even modify the chiral properties of the constituting single chiral layers. In fact, we also investigated the coupling effect between W1 and W4, which also gives rise to some extent of chirality (data not shown here), although the chirality is relatively weaker compared to the results from W2 and W3.

4. Conclusions

In conclusion, our numerical and experimental studies confirmed that chirality can be effectively achieved in a twisted double cross-wire structure. When one attempts to build bulk chiral metamaterials by the densely stacking of these double cross-wire structures, strong coupling is found between the adjacent cross-wires that belong to different unit cells. The coupling effects make the chiral properties of the stacked metamaterial different from the single chiral layers. Thus, one cannot predict the chiral behaviors of a bulk chiral metamaterial straightforwardly from the constituting single chiral layers.